Int. J. Electrochem. Sci., 13 **(2018)** 7939 – 7948, doi: 10.20964/2018.08.68

International Journal of
ELECTROCHEMICAL
SCIENCE
www.electrochemsci.org

Effect of Mn on the Characterization of Layered Perovskite $NdBaCo_{2-x}Mn_xO_{5+\delta}$ (x=0.5, 1, 1.5, 2) as Cathode Materials for IT-SOFCs

Xin Kong[1,2], *Shaoping Feng*[1, 2], *Hongyan Sun*[1,2], *Zhongzhou Yi*[1,2], *Guiyang Liu*[1,2,*]

[1] Local Characteristic Resource Utilization and New Materials Key Laboratory of Universities in Yunnan, Honghe University, Mengzi 661199, Yunnan, China.
[2] Lab of New Materials for Power Sources, College of Science, Honghe University, Mengzi 661199, Yunnan, China
[*]E-mail: liuguiyang@tsinghua.org.cn

Received: 14 April 2018 / *Accepted:* 4 June 2018 / *Published:* 5 July 2018

$NdBaCo_{2-x}Mn_xO_{5+\delta}$ (x=0.5, 1, 1.5, 2) samples are synthesized via sol-gel method. The effect of Mn on the crystal structure, thermal expansion, electrical conductivity and electrochemical properties of $NdBaCo_{2-x}Mn_xO_{5+\delta}$ (x=0.5, 1, 1.5, 2) have been investigated. The lattice parameter of $NdBaCo_{2-x}Mn_xO_{5+\delta}$ decreases when Mn increasing. The substitution of Mn for Co significantly lowers the thermal expansion coefficient (TEC) which consequently improves the mechanical compatibility with the electrolyte SDC. Although the electrical conductivity and the electrochemical performances of $NdBaCo_{2-x}Mn_xO_{5+\delta}$ (x=0.5, 1, 1.5, 2) decrease with Mn increasing, $NdBaCo_{1.5}Mn_{0.5}O_{5+\delta}$ and $NdBaCoMnO_{5+\delta}$ have better electrochemical performance and the R_p are 0.07Ωcm^2 and 0.10Ωcm^2 at 800°C respectively, which can accord with the electrochemical performance requirement of IT-SOFCs cathode materials. $NdBaCoMnO_{5+\delta}$ provides a tradeoff relationship between TEC and electrochemical performance.

Keywords: IT-SOFCs; cathode; thermal expansion coefficient; electrochemical performance.

1. INTRODUCTION

Solid Oxide Fuel Cells (SOFCs) is considered as one of the most feasible solutions for the future energy and environmental crises which have relatively higher efficiency of conversion than other traditional technologies [1, 2]. $LaMnO_3$ are widely used as traditional cathodes. However, the high operating temperature (above 1000°C) leads to some problems, such as crack formation between electrode and electrolyte due to the mismatch of thermal expansion coefficient (TEC) of the cell component, the serious interface reaction that the electrochemical properties may be deteriorated[3, 4].

Therefore the development of intermediate-temperature solid oxide fuel cells (IT-SOFCs) which operating temperature is below 800°C has received considerable interest in recent years. Intermediate operating temperature is conducive to extend the choices of the electrode materials and interconnects, reduce the production cost, enhance the stability and increase the battery lifespan [5-7]. However, the electrochemical activity of traditional ABO_3-type manganese perovskite cathode decreases dramatically during the intermediate operating temperatures[6]. Thus, researchers make great efforts to develop new mixed ionic and electronic conducting (MIEC) oxides with high catalytic activity as IT-SOFCs electrode materials.

MIEC oxides $LnBaCo_2O_{5+\delta}$ (Ln=lanthanide) have gained great attention due to their attractive electrochemical activity [8-10]. Layered perovskite oxides $LnBaCo_2O_{5+\delta}$ have rapid oxygen exchange and fast oxygen diffusion characteristics owing to their consecutive layer structure $[LnO_\delta]$-$[CoO_2]$-[BaO]-$[CoO_2]$ [5]. The surface exchange coefficient *K* and the chemical diffusion coefficient *D* in $LnBaCo_2O_{5+\delta}$ are much higher than these of ABO_3-type perovskite [11]. However, similar with other cobalt-based oxides, the TECs of $LnBaCo_2O_{5+\delta}$ are ~20×10^{-6} K^{-1} which are much higher than that of traditional electrolyte SDC ($12.2\times10^{-6}K^{-1}$)[8, 12]. The mismatch TEC between cathode and electrolyte may lead to the crack formation which shortens the lifespan of SOFCs. Therefore, it's necessary to develop novel layered perovskite cathodes with tradeoff properties between TEC and electrochemical performance.

The thermal expansion properties can be improved by partial substitution of other transition metals, such as Ni, Fe, Cu and Mn for Co[10, 12-16]. Manganese oxides are inexpensive and environmental friendly which is convenient for the large-scale development as SOFCs cathodes. Recently, the minor replacement of Co by Mn in $PrBaCo_{2-x}Mn_xO_{5+\delta}$(x = 0.1, 0.2 and 0.3) and $NdBa_{0.5}Sr_{0.5}Co_{2-x}Mn_xO_{5+\delta}$ (x = 0, 0.25, and 0.5), the partly substitution of Mn and Mg for Co in $SmBaCo_{2-x-y}Mn_xMg_yO_{5+\delta}$ (x=0.5, 1, 1.5 and y=0.05, 0.1) have been investigated in previously researches [12, 15, 16]. However, Mn-doped $NdBaCo_2O_{5+\delta}$ cathodes have not been reported so far. Co partially substituted by Mn in $NdBaCo_2O_{5+\delta}$ may offer a trade-off between electrochemical performance and TEC. With the aims of lowering the TEC and maximizing the electrochemical performance, we investigate the synthesis and characterization of $NdBaCo_{2-x}Mn_xO_{5+\delta}$ (x=0.5, 1, 1.5, 2) as cathode materials for IT-SOFCs in this research. The effect of Mn substitution for Co on structural characteristics, thermal expansion behavior, electrical properties and electrochemical performance of $NdBaCo_{2-x}Mn_xO_{5+\delta}$ (x=0.5, 1, 1.5, 2) are investigated.

2. EXPERIMENTAL

The $NdBaCo_{2-x}Mn_xO_{5+\delta}$ (x=0.5, 1, 1.5, 2) perovskite oxides were synthesized by sol-gel method. EDTA and citric acid were complexing agents and dissolved in deionized water. Nitrates $Nd(NO_3)_3\cdot6H_2O$, $Ba(NO_3)_2$, $Co(NO_3)_2\cdot6H_2O$ and $Mn(NO_3)_2$ were the metal sources. The mole ratio of citric acid and EDTA to the total metal ions in the final solution was 1.5:1:1. In water bath, the solutions were mixed thoroughly at 80°C. Assistant reagent $NH_3\cdot H_2O$ was added to adjust the pH

value to 7. The gel was dried in drying oven to obtain precursors and then the precursors were sintered in air at 1100°C for 10h to obtain the cathodes powders.

The electrolyte powder of $Sm_{0.2}Ce_{0.8}O_{2-\delta}$(SDC) was synthesized by the conventional solid reaction method using dried starting materials Sm_2O_3 and CeO_2. The as-synthesized SDC powders were sintered in air at 1200°C for 5 h. Uniaxially pressed SDC electrolytes with PVA agglomerant were sintered at 1450°C for 2h to obtain SDC electrolyte disks. The dense SDC electrolyte were fabricated to characterize the electrochemical performance of the cathodes.

The ink for electrode deposition was prepared by mixing the as-prepared $NdBaCo_{2-x}Mn_xO_{5+\delta}$ (x=0.5, 1, 1.5, 2) powder with ethylcellulose and terpinol in appropriate ratio. The cathode slurry was applied on both sides of SDC electrolyte disks with circle pattern as working electrode (WE) and opposite side with same surface area as counter electrode (CE). The disks were sintered at 1000℃ for 2h in air. And current collectors of silver pastes were further coated onto the surfaces of electrodes. The disks were sintered at 700℃ for 30 minutes in air to form symmetrical configuration for the electrochemical performance measurement.

The synthesized cathodes $NdBaCo_{2-x}Mn_xO_{5+\delta}$ (x=0.5, 1, 1.5, 2) were characterized by X-ray diffraction (XRD),The phase analyses of powders was evaluated by X-ray diffraction using PANalytical X'Pert Powder X-ray Diffractometer. $NdBaCo_{2-x}Mn_xO_{5+\delta}$ (x=0.5, 1, 1.5, 2) oxides mixed PVA agglomerant evenly were pressed and heated at 1150°C, 1200°C, 1250℃ for 2h to form dense samples to measure the electrical properties and TEC performance. The electrical conductivities of $NdBaCo_{2-x}Mn_xO_{5+\delta}$ (x=0.5, 1, 1.5, 2) samples were measured with a four-probe dc method using ST-2258C four point probes meter from 50°C to 800°C. The TECs of $NdBaCo_{2-x}Mn_xO_{5+\delta}$ (x=0.5, 1, 1.5, 2) were measured by ZRPY-1000 thermal dilatometer from room temperature to 800°C with a heating rate of 5°C/min. The electrochemical performance of $NdBaCo_{2-x}Mn_xO_{5+\delta}$ (x=0.5, 1, 1.5, 2) cathodes were measured at different temperatures by ac-impedance spectroscopy using an electrochemical workstation CHI604D from 0.1 Hz to 10^5 Hz with the amplitude potential of 10 mV. The electrochemical impedance data were fitting by the ZSimpWin software.

3. RESULTS AND DISCUSSION

3.1 XRD analysis

The X-ray diffraction patterns of $NdBaCo_{2-x}Mn_xO_{5+\delta}$ (x=0.5, 1, 1.5, 2) sintered at 1100°C for 10h is shown in Fig.1. The characteristic peaks of $NdBaCo_{2-x}Mn_xO_{5+\delta}$ (x=0.5, 1, 1.5, 2) are layered perovskites [17], but impure peaks are observed in $NdBaCo_{0.5}Mn_{1.5}O_{5+\delta}$ at 31.2°and $NdBaMn_2O_{5+\delta}$ at 30.7°, respectively. When the content of manganese increase from 0.5 to 2, it's observed the characteristic peaks of $NdBaCo_{2-x}Mn_xO_{5+\delta}$ (x=0.5, 1, 1.5, 2) shift slightly from low angle to the high angle which indicates a reduction of lattice parameter. This is due to the substitution of Mn with larger ion radius for Co with smaller ion radius (Mn^{3+}: 0.058 nm for low spin and 0.065 nm for high spin, Mn^{4+}: 0.053 nm; Co^{3+}: 0.055 nm for low spin and 0.061 nm for high spin, Co^{4+}: 0.053 nm)[16].

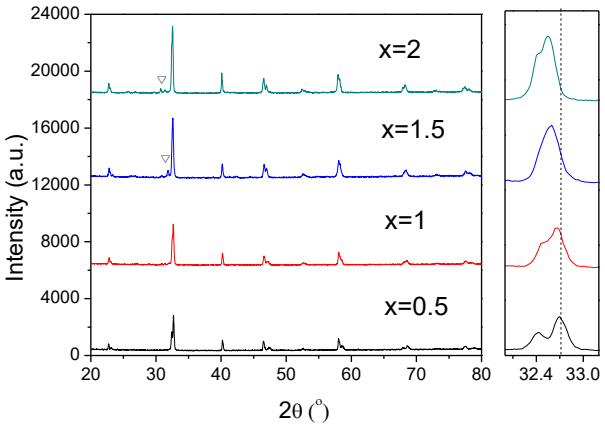

Figure 1. The X-ray diffraction patterns of $NdBaCo_{2-x}Mn_xO_{5+\delta}$ (x=0.5, 1, 1.5, 2) sintered at 1100°C for 10h.

3.2 Thermal expansion behavior

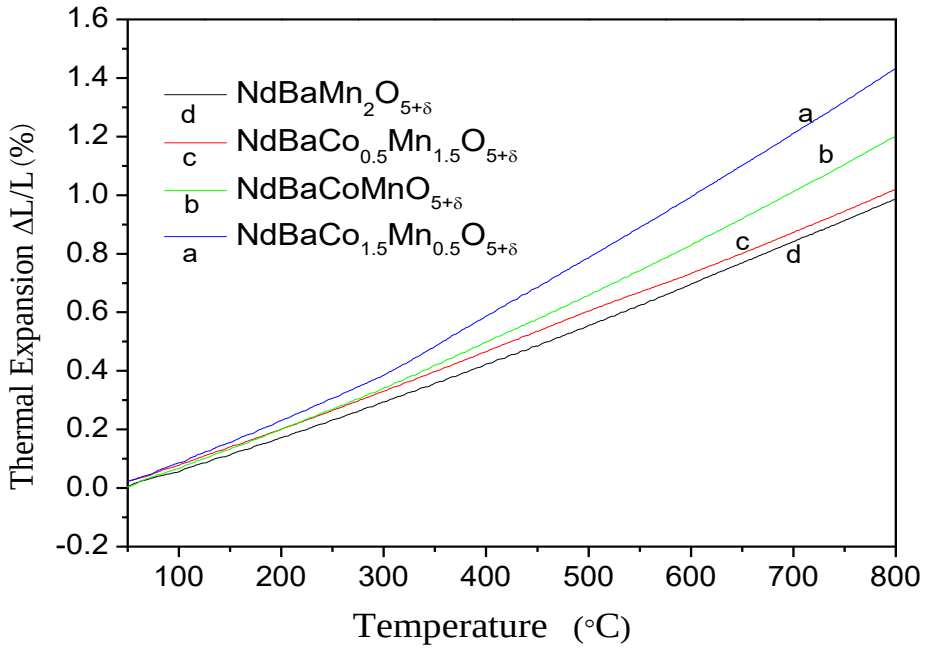

Figure 2. The thermal-expansion ($\Delta L/L_0$) curves of $NdBaCo_{2-x}Mn_xO_{5+\delta}$ (x=0.5, 1, 1.5, 2) from room temperature to 800 °C.

Fig.2 shows the thermal-expansion ($\Delta L/L_0$) curves of $NdBaCo_{2-x}Mn_xO_{5+\delta}$ (x=0.5, 1, 1.5, 2) from room temperature to 800 °C. The average TEC of $NdBaCo_{1.5}Mn_{0.5}O_{5+\delta}$, $NdBaCoMnO_{5+\delta}$, $NdBaCo_{0.5}Mn_{1.5}O_{5+\delta}$ and $NdBaMn_2O_{5+\delta}$ are 18.86×10^{-6}/°C, 15.59×10^{-6}/°C, 12.89×10^{-6}/°C and 12.8×10^{-6}/°C, respectively. The TEC value of $NdBaCo_{2-x}Mn_xO_{5+\delta}$ (x=0.5, 1, 1.5, 2) reduces with Mn increasing. The substitution of manganese for cobalt lowers the TEC of Co-based layered perovskites. The result suggests that the TEC of $NdBaCo_{2-x}Mn_xO_{5+\delta}$ (x=1, 1.5, 2) are more compatible with that of traditional

electrolyte SDC ($12.20\times10^{-6}K^{-1}$[8]) and are much lower than these of Co-based layered perovskites, such as $NdBa_{0.5}Sr_{0.5}CoO_{5+\delta}$ ($20.27\times10^{-6}K^{-1}$) [8], $SmBaCo_2O_{5+\delta}$ ($21.2\times10^{-6}K^{-1}$)[14] and $PrBaCo_{1.9}Mn_{0.1}O_{5+\delta}$ ($22.8\times10^{-6}K^{-1}$)[15]. Cobalt-based layered perovskites suffer the abnormally high TEC due to Co^{3+} transition from low-spin to high-spin with temperature [8, 15, 16]. The TEC of manganese-based layered perovskites significantly decreases owing to the suppression of the spin state transition of Co^{3+} which consequently improves the mechanical compatibility with the electrolyte SDC.

3.3 Electrical conductivity

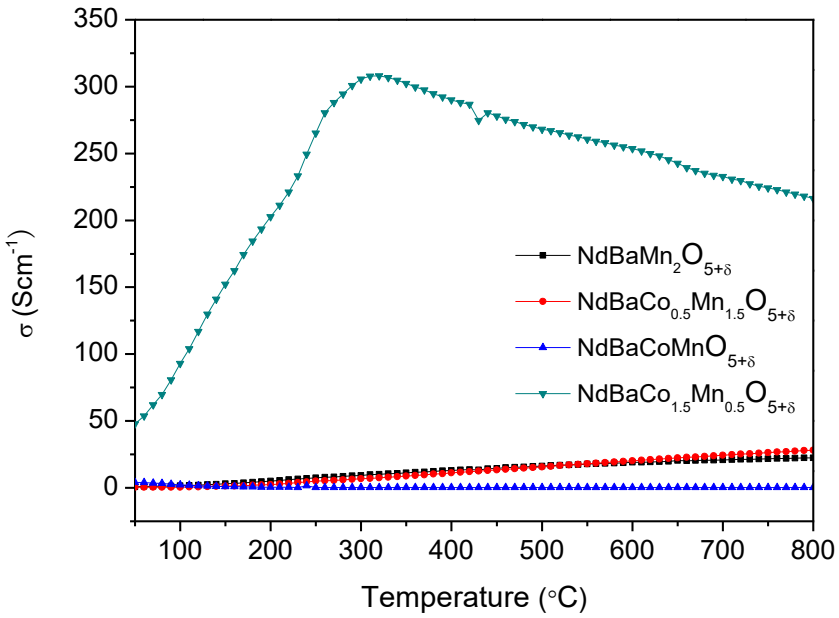

Figure 3. Temperature dependence of electrical conductivity of $NdBaCo_{2-x}Mn_xO_{5+\delta}$ (x=0.5, 1, 1.5, 2) samples from 50 °C to 800 °C in air.

Fig.3 shows the temperature dependence of electrical conductivity of $NdBaCo_{2-x}Mn_xO_{5+\delta}$ (x=0.5, 1, 1.5, 2) samples from 50 °C to 800 °C in air. The electrical conductivity of $NdBaCo_{1.5}Mn_{0.5}O_{5+\delta}$ shows a typical semiconductor to metal-conductor transition. The same phenomena occur in other layered perovskites oxides [3, 8]. In the temperature range of 50-307°C, the conductivity of $NdBaCo_{1.5}Mn_{0.5}O_{5+\delta}$ increases gradually with temperature increasing and shows a typical semiconductor behavior which can be ascribed to thermal-activation of electronic hopping[15]. The maximum conductivity is 216 Scm^{-1} at 307°C. In the temperature range of 307-800°C, the conductivity of $NdBaCo_{1.5}Mn_{0.5}O_{5+\delta}$ decreases with temperature increasing and shows a metallic behavior which is closely associated with the more charge carriers annihilation. The Lattice oxygen loses with temperature increasing. More oxygen vacancies are formed, accompanied with a reduction of Co^{4+} or Mn^{4+} to Co^{3+} or Mn^{3+} during higher temperatures[15]. The concentration of the charge carrier is decreased, consequently[16]. As the defect reaction represented in Eq.1

$$2Co_{Co}^{\bullet} + O_O^{\times} = 1/2O_2(g) + V_O^{\bullet\bullet} + 2Co_{Co}^{\times} \quad \text{Eq.1}$$

Where $O_O^{\times}$ and $V_O^{\bullet\bullet}$ represent oxygen ions and oxygen vacancies respectively. Beside, the primary charger carriers are transported by the Co-O-Co network. The randomly distributed oxygen vacancies perturbs the (Co, Mn)–O–(Co, Mn) periodic potential so that it leads to the carrier localization [12]. The conductivity of $NdBaCo_{2-x}Mn_xO_{5+\delta}$ (x=1, 1.5, 2) samples increases gradually with temperature increasing due to an increase of thermal-activation of electronic hopping [13]. However, metal–insulator transition (MIT) behaviors have not been observed in them. The maximum conductivity of $NdBaCo_{2-x}Mn_xO_{5+\delta}$ (x=1, 1.5, 2) is 4.05 Scm^{-1}, 28.14 Scm^{-1} and 22.50 Scm^{-1} at 800°C, respectively. The electrical conductivity of $NdBaCo_{2-x}Mn_xO_{5+\delta}$ (x=1, 1.5, 2) decreases when the Mn content increasing, mainly due to the decrease in the overlap between the (Co, Mn):3d orbital and O:2p orbital which causes the covalency of the (Co, Mn) -O- (Co, Mn) bond decreases [12, 18, 19]. The maximum conductivity of $NdBaCo_{2-x}Mn_xO_{5+\delta}$ (x=1, 1.5, 2) are in the same order with other free-Cobalt based layered perovskites, such as $NbBaCu_2O_{5+\delta}$(16.87 Scm^{-1} at 560 °C) [8], $SmBaCu_2O_{5+\delta}$ (31.61 Scm^{-1} at 610 °C) [14].

3.4 Electrochemical properties

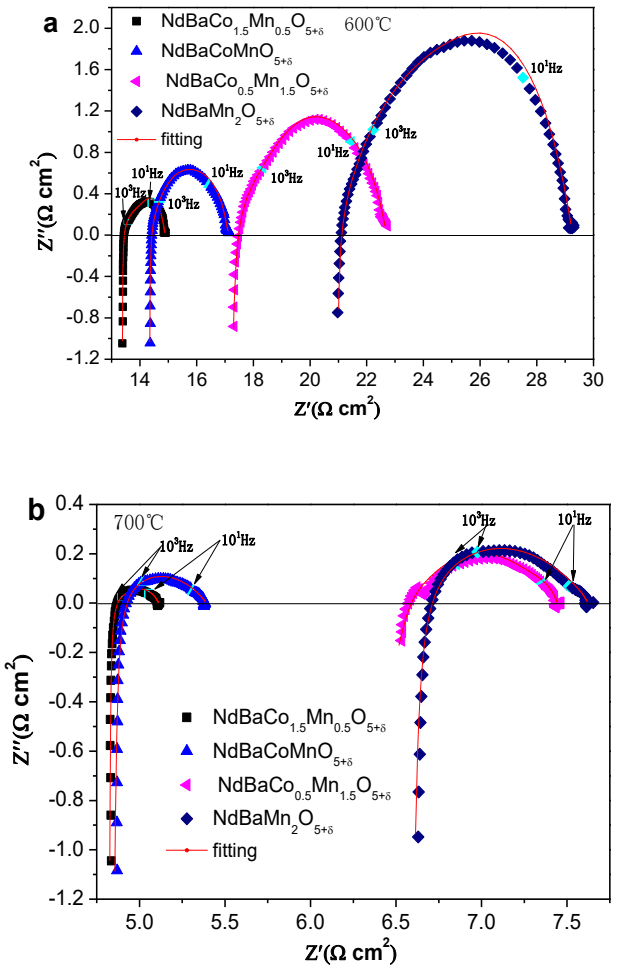

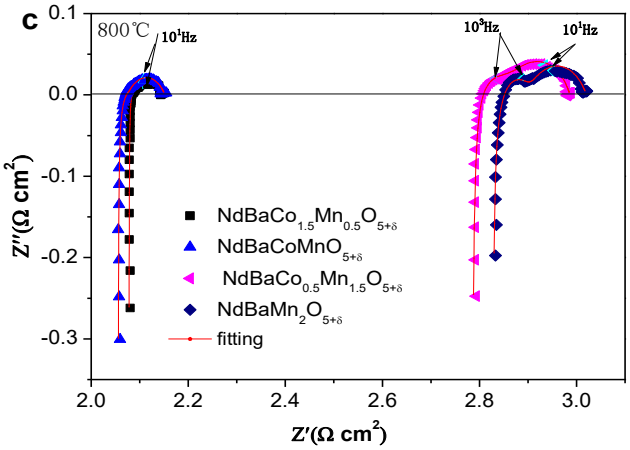

Figure 4. Impedance spectra of $NdBaCo_{2-x}Mn_xO_{5+\delta}$ (x=0.5, 1, 1.5, 2) in air at (a) 600°C, (b)700 °C and (c)800°C.

The electrochemical performance of the $NdBaCo_{2-x}Mn_xO_{5+\delta}$ (x=0.5, 1, 1.5, 2) are tested on symmetrical cells NBCMO/SDC/NBCMO by means of EIS. Impedance spectra of $NdBaCo_{2-x}Mn_xO_{5+\delta}$ (x=0.5, 1, 1.5, 2) in air are shown in Fig.4. In order to investigate the process of oxygen reduction reaction (ORR) of $NdBaCo_{2-x}Mn_xO_{5+\delta}$ (x=0.5, 1, 1.5, 2), the impedance spectra are analyzed by fitting equivalent circuit models using ZSimpWin software. The Nyquist impedance spectra of $NdBaCo_{2-x}Mn_xO_{5+\delta}$ (x=0.5, 1, 2) are fitted well by the equivalent circuit model $LR_{el}(Q_1R_1)(Q_2R_L)$ and the Nyquist impedance spectra of $NdBaCo_{0.5}Mn_{1.5}O_{5+\delta}$ are fitted well by the equivalent circuit model $LR_{el}(Q_1R_1)(Q_2R_2)(Q_3R_L)$. The R_{el} at high frequency intercepted with the real axis R_{el} denotes the ohmic resistance which includes the resistance contributions of the electrolyte, the electrodes, the current collectors and the lead wires. L denotes a high frequency induction tail ascribed to the device and connects leads; Q represents a nonideal capacitor. The fitting results indicate that there are at least two electrode processes corresponding to the high and low frequency arcs during ORR. R_1 and R_2 are equivalent to the high frequency polarization resistances R_H which are caused by the charge transfer during the migration and diffusion of oxygen ions from the triple phase boundaries (TPB) into electrolyte lattice. R_L is relative to the low frequency polarization resistance which is associated with the adsorption/desorption of the molecular oxygen, bulk or surface oxygen diffusion process [3, 12]. The total polarization resistance R_p is defined by the sum of resistances R_H and R_L.

The EIS fitting results of $NdBaCo_{2-x}Mn_xO_{5+\delta}$ (x=0.5, 1, 1.5, 2) cathode measured in air at 600°C, 700°C, 800°C are shown in Table 1-3, respectively. In 600-800°C, the R_2 of $NdBaCo_{2-x}Mn_xO_{5+\delta}$ (x=0.5, 1, 1.5, 2) are larger than R_1, which was interpreted the oxygen diffusion processes are the rate-determining step of ORR. At the same temperature, Both R_H and R_L increase with Mn increasing, due to the increase in the number of low spins Mn^{3+} which traps oxygen vacancies [10, 12]. The oxygen exchange and the transport speed of oxide ions reduce consequently. Besides, with Mn increasing, the overlap between the (Co,Mn):3d orbital and O:2p orbital reduce which leads to the reduction of charge transfer [10, 16, 20].

Although electrochemical performances of $NdBaCo_{2-x}Mn_xO_{5+\delta}$ (x=0.5, 1, 1.5, 2) decreases with Mn increasing, the R_p of $NdBaCo_{0.5}Mn_{1.5}O_{5+\delta}$ and $NdBaCoMnO_{5+\delta}$ are 0.07Ωcm^2 and 0.10Ωcm^2 at 800°C which are much lower than that of Manganese-based perovskite, such as $La_{0.8}Sr_{0.2}Co_{0.17}Mn_{0.83}O_{3-\delta}$ (2.4Ωcm^2 at 800°C)[21], $Sm_{0.5}Sr_{0.5}MnO_3$ (1.92Ωcm^2 at 800°C)[22], $PrBaCo_{1.9}Mn_{0.1}O_{5+\delta}$ (0.16Ωcm^2 at 800°C) [15] and $PrBaCo_{1.7}Mn_{0.3}O_{5+\delta}$ (0.15Ωcm^2 at 800°C)[15] . $NdBaCo_{0.5}Mn_{1.5}O_{5+\delta}$ and $NdBaCoMnO_{5+\delta}$ can accord with the requirement of electrochemical performance of IT-SOFC cathode materials.

Table 1. EIS fitting results of $NdBaCo_{2-x}Mn_xO_{5+\delta}$ (x=0.5, 1, 1.5, 2) cathode measured in air at 600 °C.

Mn	L	R_{el}	R_H		R_L	R_p
	(Hcm^2)	(Ωcm^2)	R_1 (Ωcm^2)	R_2 (Ωcm^2)	(Ωcm^2)	(Ωcm^2)
0.5	2.012E-6	13.36	0.66	-	0.87	1.53
1	2.054E-6	14.32	0.57	-	2.24	2.81
1.5	2.075E-6	17.06	1.72	1.28	2.64	5.64
2	1.629E-6	20.88	2.92	-	5.48	8.40

Table 2. EIS fitting results of $NdBaCo_{2-x}Mn_xO_{5+\delta}$ (x=0.5, 1, 1.5, 2) cathode measured in air at 700 °C.

Mn	L	R_{el}	R_H		R_L	R_p
	(Hcm^2)	(Ωcm^2)	R_1 (Ωcm^2)	R_2 (Ωcm^2)	(Ωcm^2)	(Ωcm^2)
0.5	2.026E-6	4.82	0.10	-	0.20	0.30
1	2.136E-6	4.72	0.11	-	0.56	0.67
1.5	6.501E-7	6.66	0.0001	0.13	0.65	0.78
2	1.894E-6	6.56	0.01	-	1.05	1.06

Table 3. EIS fitting results of $NdBaCo_{2-x}Mn_xO_{5+\delta}$ (x=0.5, 1, 1.5, 2) cathode measured in air at 800 °C.

Mn	L	R_{el}	R_H		R_L	R_p
	(Hcm^2)	(Ωcm^2)	R_1 (Ωcm^2)	R_2 (Ωcm^2)	(Ωcm^2)	(Ωcm^2)
0.5	5.044E-7	2.08	0.03	-	0.04	0.07
1	5.808E-7	2.06	0.02	-	0.08	0.10
1.5	4.875E-7	2.78	9.973E-6	0.11	0.10	0.21
2	3.905E-7	2.83	0.08	-	0.12	0.20

4. CONCLUSIONS

In order to develop novel layered perovskite oxides with lower TEC and adequate electrochemical activity, $NdBaCo_{2-x}Mn_xO_{5+\delta}$ (x=0.5, 1, 1.5, 2) are synthesized via citrate-EDTA sol-gel method. Although the substitution of Mn for Co leads to a decrease in electrical conductivity, the TEC becomes more compatible with SDC electrolyte due to the suppression of Co^{3+} transition from low-spin to high-spin. The TEC of $NdBaCo_{1.5}Mn_{0.5}O_{5+\delta}$, $NdBaCoMnO_{5+\delta}$, $NdBaCo_{0.5}Mn_{1.5}O_{5+\delta}$ and $NdBaMn_2O_{5+\delta}$ are 18.86×10^{-6}/°C, 15.59×10^{-6}/°C, 12.89×10^{-6}/°C and 12.8×10^{-6}/°C, respectively. $NdBaCo_{1.5}Mn_{0.5}O_{5+\delta}$ and $NdBaCoMnO_{5+\delta}$ have better electrochemical performance, the R_p are $0.07\Omega cm^2$ and $0.10\Omega cm^2$ at 800°C. Among the samples, the $NdBaCoMnO_{5+\delta}$ show better tradeoff properties between TEC and electrochemical performance as a promising cathode material for IT-SOFCs.

ACKNOWLEDGEMENTS
This work was supported by the Yunnan Applied Basic Research Project (No.2017FD157), the National Natural Science Foundation of China (No.51662007 and No.U1602273), Yunnan Local Colleges (part) Applied Basic Projects Joint Special Foundation (No.2017FH001-120).

References

1. O.L. Pineda, Z.L. Moreno, P. Roussel, K. Świerczek and G.H. Gauthier, *Solid State Ionics*, 288 (2016) 61-67.
2. N.Q. Minh, *Solid State Ionics*, 174 (2004) 271-277.
3. X. Ding, X. Kong, H. Wu, Y. Zhu, J. Tang and Y. Zhong, *International Journal of Hydrogen Energy*, 37 (2012) 2546-2551.
4. X. Ding, X. Kong, J. Jiang, C. Cui and L. Guo, *International Journal of Hydrogen Energy*, 35 (2010) 1742-1748.
5. B. Wei, Z. Lü, T. Wei, D. Jia, X. Huang, Y. Zhang, J. Miao and W. Su, *International Journal of Hydrogen Energy*, 36 (2011) 6151-6159.
6. X. Zhu, H. Xia, Y. Li and Z. Lü, *Materials Letters*, 161 (2015) 549-553.
7. R.A. De Souza, J.A. Kilner and J.F. Walker, *Materials Letters*, 43 (2000) 43-52.
8. X. Kong, G. Liu, Z. Yi and X. Ding, *International Journal of Hydrogen Energy*, 40 (2015) 16477-16483.
9. A. Jun, T.-h. Lim, J. Shin and G. Kim, *International Journal of Hydrogen Energy*, 39 (2014) 20791-20798.
10. J.H. Kim and A. Manthiram, *Electrochimica Acta*, 54 (2009) 7551-7557.
11. A.A. Taskin, A.N. Lavrov and Y. Ando, *Applied Physics Letters*, *86* (2005) 091910
12. X. Kong, H. Sun, Z. Yi, B. Wang, G. Zhang and G. Liu, *Ceramics International*, 43 (2017) 13394-13400.
13. L. Jiang, T. Wei, R. Zeng, W.-X. Zhang and Y.-H. Huang, *Journal of Power Sources*, 232 (2013) 279-285.
14. X. Kong and X. Ding, *International Journal of Hydrogen Energy*, 36 (2011) 15715-15721.
15. W. Guo, R. Guo, L. Liu, G. Cai, C. Zhang, C. Wu, Z. Liu and H. Jiang, *International Journal of Hydrogen Energy*, 40 (2015) 12457-12465.
16. J. Kim, S. Choi, S. Park, C. Kim, J. Shin and G. Kim, *Electrochimica Acta*, 112 (2013) 712-718.
17. T.V. Aksenova, L.Y. Gavrilova, A.A. Yaremchenko, V.A. Cherepanov and V.V. Kharton, *Materials Research Bulletin*, 45 (2010) 1288-1292.

18. A. Jun, T.H. Lim, J. Shin and G. Kim, *International Journal of Hydrogen Energy,* 39 (2014) 20791-20798.
19. K.T. Lee and A. Manthiram, *Solid State Ionics,* 178 (2007) 995-1000.
20. S. Choi, J. Shin, K.M. Ok and G. Kim, *Electrochimica Acta,* 81 (2012) 217-223.
21. Y. Bai, M. Liu, D. Ding, K. Blinn, W. Qin, J. Liu and M. Liu, *Journal of Power Sources,* 205 (2012) 80-85.
22. W. Li, J. Pu, B. Chi and L. Jian, *Electrochimica Acta,* 141 (2014) 189-194.